New Horizons in Earth Reinforcement – Otani, Miyata & Mukunoki (eds)
© 2008 Taylor & Francis Group, London, ISBN 978-0-415-45775-0

Numerical assessment of the performance of protecting wall against rockfall

E. Sung, A. Yashima, D. Aminata & K. Sugimori
Dept. of Civil Engr., Gihu University, Gihu, Japan

K. Sawada
River Basin Research Center, Gifu University, Gihu, Japan

S. Inoue & Y. Nishida
Protech Engineering Co. Ltd., Niigata, Japan

ABSTRACT: We have to reduce the disaster caused by rockfall as well as conserve the surrounding environment. In order to satisfy these requirements, we have proposed new construction methods, which use on-site ground materials. Full-scale field tests have been performed by some of the authors. Three different types of protecting walls were constructed on the test site, type 1: the dyke-type wall composed of geo-grid reinforcement and soil, type 2: vertical wall composed of cast iron-panel and boulders, and type 3: vertical wall composed of wooden-panel and soil. It has been confirmed based on the full-scale tests that newly proposed protecting walls have a certain degree of potential with respect to the energy absorption against rockfall impact. However, the stability of the protecting walls against larger impacts has not been investigated yet. Therefore, in this study, a series of dynamic finite element analyses (LS-DYNA) were carried out in order to understand the details of stability of different types of protecting walls against larger impacts by falling rock. Firstly, the energy absorption during the full-scale tests was reproduced by employing an appropriate constitutive model for wall structures. Then, the stress, deformation and failure inside the wall by the larger impact forces than the observed in the field tests were discussed based on the numerical results. The efficiency of three types of protecting walls against rockfall is found to be quantitatively.

1 INTRODUCTION

A rockfall is a high frequency unexpected disaster among the slope disasters and has an effect on the road, railway and building. The protective countermeasures against this rockfall are very expensive and difficult. Therefore, a interest of protecting wall using a ground material like soil and boulders is increasing due to a energy absorption. However, The effect of rockfall on the ground has not been fully understood.

Recently, several studies on this interaction problem have been published. Among them Prisco, & Vecchiotti (2004) published the study about a rheological model for the description of rockfall on homogeneous ground and discussed impact load against vertical falling rockfall. Wu & Thomson (2007) also presents the interaction between a guardrail post and soil during quasi-static and dynamic loading by field tests and numerical analyses using LS-DYNA.

The interaction problem between rockfall and protecting wall using ground material should consider about constitutive model of ground and shape of protecting wall. Therefore, this paper presents full-scale model tests and numerical analyses to investigate the mechanical behaviors of protecting wall using ground material during rockfall. Acceleration, penetration and impact load due to rockfall are investigated with the newly developed three kinds of protecting walls and the influences of larger impact energy and impact point in the protecting wall are also investigated by numerical analyses.

2 DESCRIPTION OF FULL-SCALE FIELD TESTS

Full-scale field tests were carried out to investigate the effects of rockfall to three kinds of protecting walls. Figure 1 is a description of these full-scale field tests and an imitation rockfall for this purpose. The imitation rockfall, a 75 cm diameter and weight of 4.9 kN, was made by concrete and freely fallen by two cranes to the protecting wall from the height of 11 m as shown Figure 1. The impact energy in this full-scale field tests

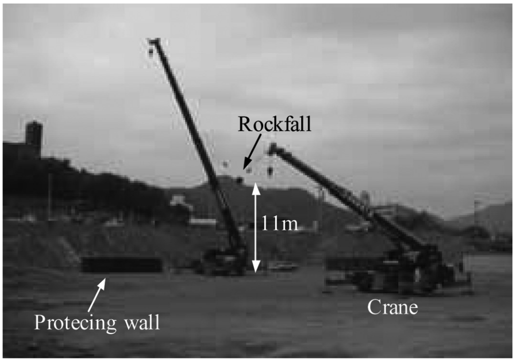

Figure 1. Description of full-scale field tests.

Figure 2. Concrete ball for rockfall and three-dimensional accelerometer.

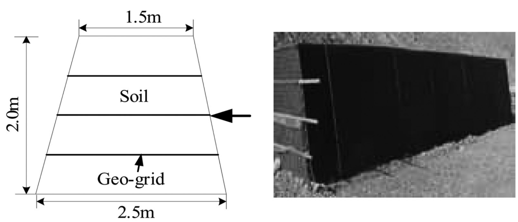

(a) Type 1

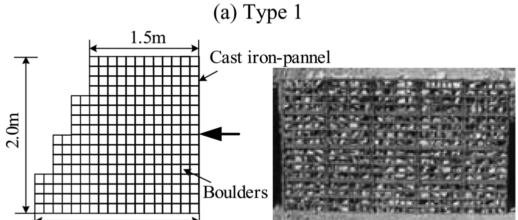

(b) Type 2

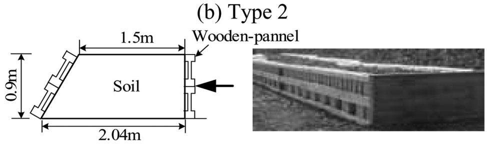

(c) Type 3

Figure 3. Three kinds of protecting walls in field tests.

is assumed to be 55.6 kJ. Acceleration of the rockfall at the moment of impact was measured continually by a three-directional accelerometer installed inside of rockfall as shown Figure 2. The measured acceleration (a, m/sec^2) was convert to the velocity v (m/sec^2), displacement u (m), load f (kN) and absorption energy Ea (kJ) by simple integration method.

Figure 3 represents three kinds of protecting walls used in the full-scale field tests. Type 1 is a dyke-type wall composed by reinforced soil with geo-grid. Type 2 is a vertical wall composed of cast iron-panel and boulders, and type 3 is a vertical wall composed of wooden-panel and soil. The heights of these protecting walls are 2 m for type 1 and 2 and 0.9 m for type 3. The length is 5 m. The rockfall is impacted at middle point in all types of protecting walls.

3 DESCRIPTION OF NUMERICAL ANALYSES

Numerical analyses by LS-DYNA (Hallquist, 2003) to investigate a deformation and stability of protecting wall is conducted in the same scale as the full-scale field tests. Figure 4 shows the 3D meshes for all types of protecting walls. Bottom faces of the 3D mesh are fixed and the other nodes are free in three directions. The geogrid, iron-cased panel and wooden panel are not considered in these analyses. All protecting walls are modeled by single material to investigate the effect between a ground material and an impact of rockfall. In order to simulate the impact of rockfall, initial velocity toward the protecting wall is applied. The initial velocity of free falling rockfall at 10 m height is about 14.76 m/s.

A concrete ball is assumed to be a rigid, and a visco-elastic (Mat_5) or elasto-perfect plastic model is used for protecting wall. The visco-elastic model can express the change on the stiffness of material according to time as following equation.

$$G = G_f + (G_i - G_f)\exp(-\beta t) \tag{1}$$

Here, G is a shear modulus at the present. Gi and G_f are initial and final shear modulus respectively. β is a change rate of shear modulus with respect to the time. Figure 5 shows a simulation of triaxial test for visco-elastic model.

The Drucker-prager model is used to investigate the plastic and residual deformation of protecting wall. This model does not consider the strain hardening, softening and strain rate effect. On the other hand, this model is easy to get the material parameter (internal friction angle and cohesion). Figure 6 represents a stress-strain relation and dilatancy for triaxial test for this model. Expansions of material begin when stress reach at failure state as shown in Figure 6b and the material with larger internal friction angle shows larger expansion than those with smaller friction angles. Model parameters for these constitutive models are fitted based on the experiment results.

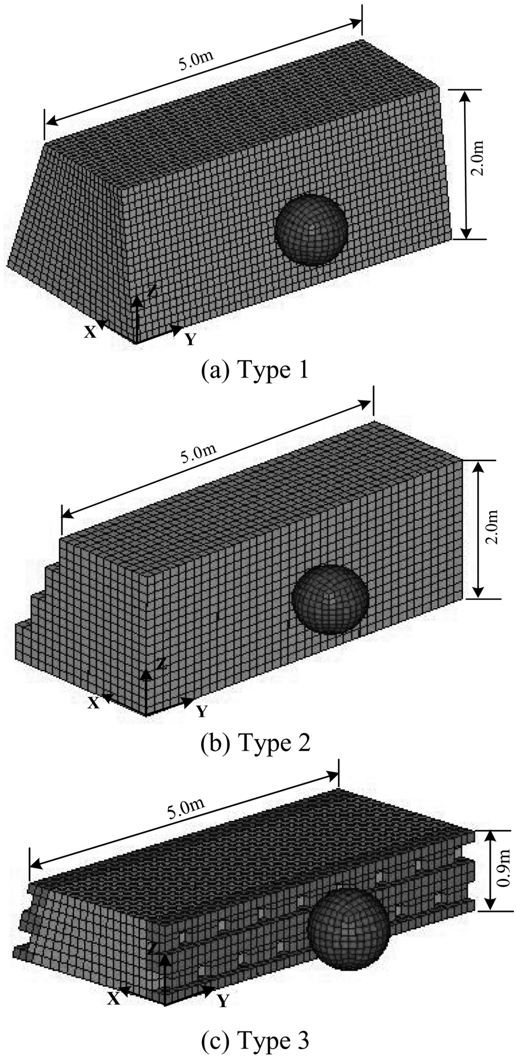

Figure 4. FEM meshes used in numerical analyses.

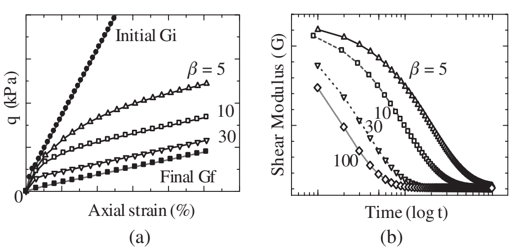

Figure 5. Results of numerical simulation for triaxial tests used in visco-elastic model (a) deviatric stress-axial strain relation (b) change of elastic modulus by time.

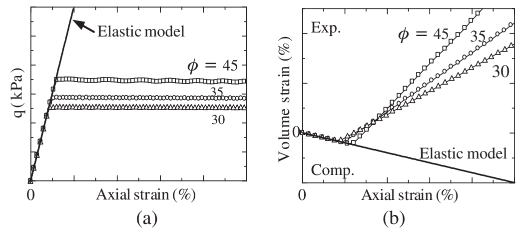

Figure 6. Results of numerical simulation for triaxial tests used in elasto-plastic model (a) deviatric stress-axial strain relation (b) dilatancy relation

Before the impact load is applied, the initial stress condition of a protecting wall are calculated by body forces to all elements under gravitational condition. The contact condition between rockfall and protecting wall is simulated by penalty method in LS-DYNA. The static and dynamic friction angle at the interface between rockfall and a protecting wall is assumed to be 35°.

4 RESULTS AND DISCUSSION

4.1 *Results of full-scale field tests*

Figure 7 shows the results of full-scale field tests for three kinds protecting walls. Type 1 composed by reinforced soil with geogrid represents the largest value of acceleration and impact load of rockfall among these three kinds of walls. The penetration amount of rockfall toward protecting wall for type 1 is smaller than other walls. This means that the stiffness of type 1 is the largest in three walls. The penetration amount of rockfall toward protecting wall for type 1 is smaller than other walls. This means that the stiffness of type 1 is the largest in three walls. On the other hands, the acceleration and impact load of rockfall of type 2 and 3 show lower values than type 1 because the deformations of wall in type 2 and 3 is larger than type 1 for the same impact energy. However, the repair of these protecting walls with soil and boulders is easy compared with concrete wall or steel frame type walls after rockfall.

4.2 *Comparisons between field tests and numerical analyses*

Firstly, the elastic analyses using various elastic moduli are carried out to get the initial elastic parameter of protecting wall by the comparison with test results. Figure 8 shows the acceleration time histories for type 1 according to various Young's moduli. All results of elastic analyses are different from test result. On the other hand, in the case of $E = 3.0E + 07$ Pa, the initial slope of acceleration curve is fit to the experiment.

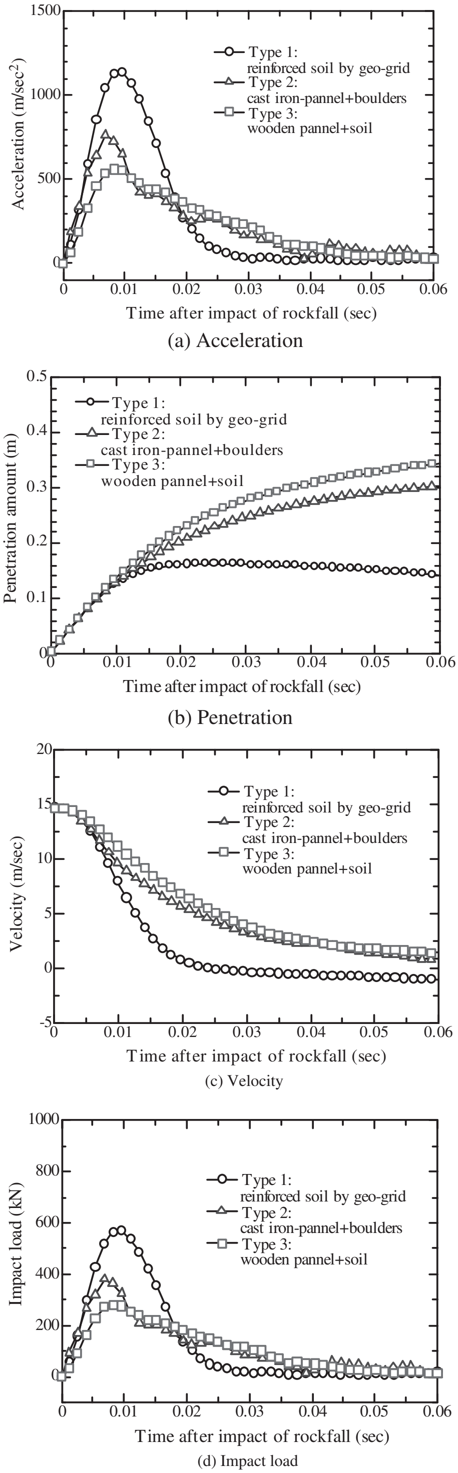

Figure 7. Results of full-scale field tests.

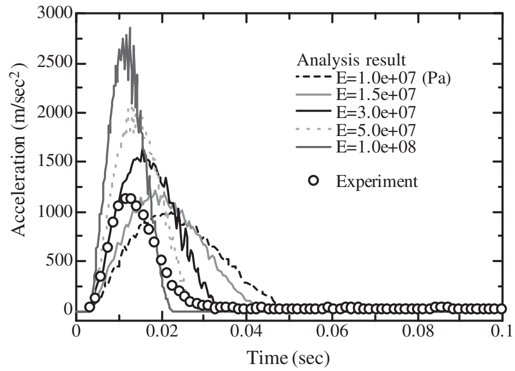

Figure 8. Elastic analyses of type 1 by various elastic constants.

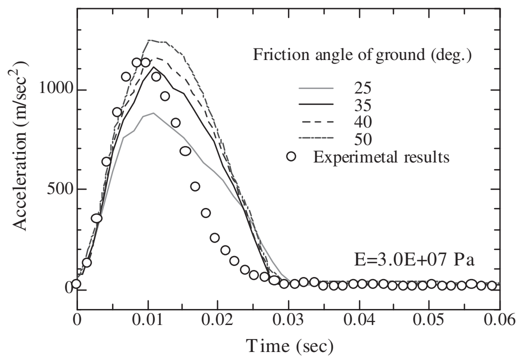

Figure 9. Elasto-plastic analyses for type 1 by various friction angles with E = 3.0E + 07 Pa.

Therefore, This Young's modulus is selected to all analyses for type 1. Those of type 2 and 3 are determined through this method.

Figure 9 shows the acceleration for type 1 by various internal friction angles. The internal friction angle, 35°, is selected due to the best fit to the test result. Parameters for another types are also decided by this way. The selected Young's modulus and friction angle are much smaller than those of usual soil and boulders. However, these parameters have been used to know the impact load and displacement of rockfall by numerical analyses.

Figure 10 represents the impact load with respect to time from numerical analyses and experiments for three kinds of protecting walls.

In these figures, three constitutive models (elastic, visco-elastic and elasto-perfectly plastic model) are indicated to compare with experiment results.

As shown in these figures, the impact load with visco-elastic and elasto-plastic model for protecting wall is well fit to those of experiments. The difference at the parts of descending curve after the maximum

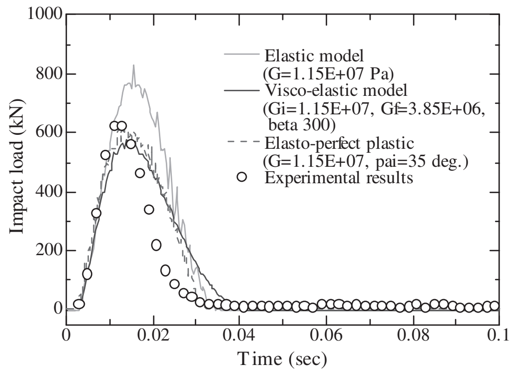

(a) Type 1

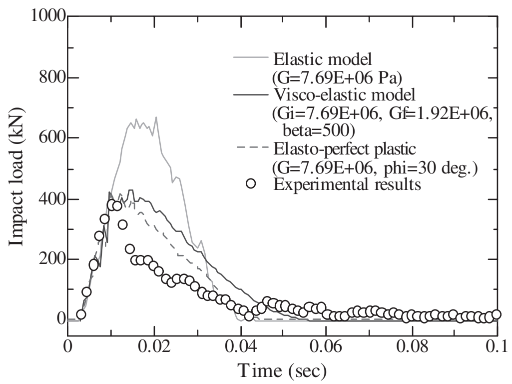

(b) Type 2

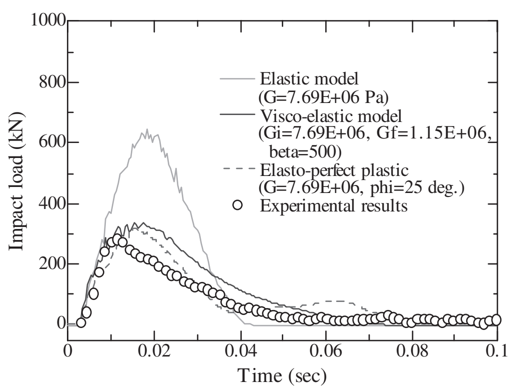

(c) Type 3

Figure 10. Comparisons with impact load of rockfall between numerical analyses and tests.

impact load is due to the leading cable that connected to the rockfall and crane car.

The penetration amount of rockfall for three types by numerical analyses and experiment is represented

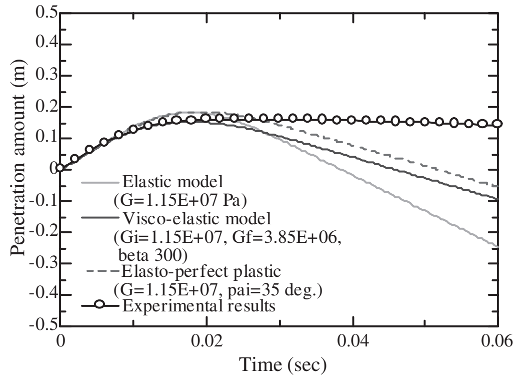

(a) Type 1

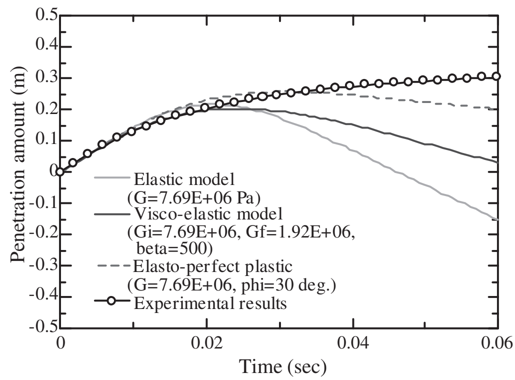

(b) Type 2

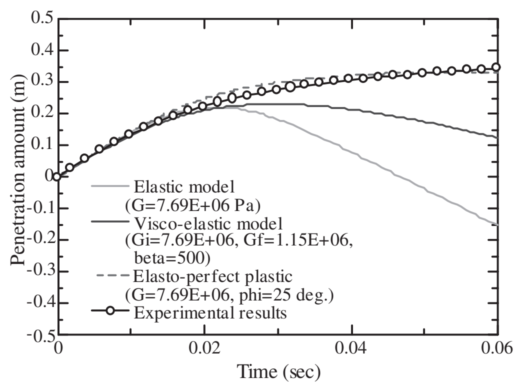

(c) Type 3

Figure 11. Comparisons with penetration amount between numerical analyses and tests.

in Figure 11. Although the maximum interpenetration amount of rockfall into the protecting wall is same to those of experiment results in the case of type 1 in all-material models, the difference between numerical analyses and test after peak penetration become larger with time.

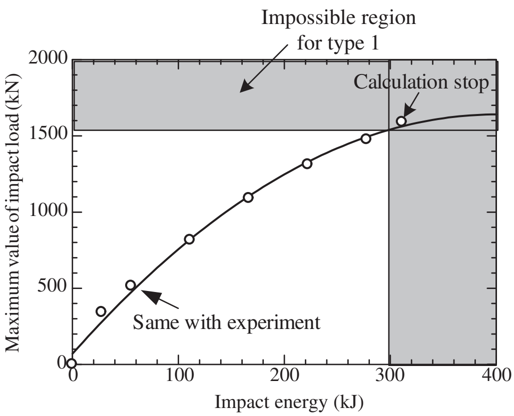

Figure 12. Calculated the maximum impact load of rockfall according to given impact energy.

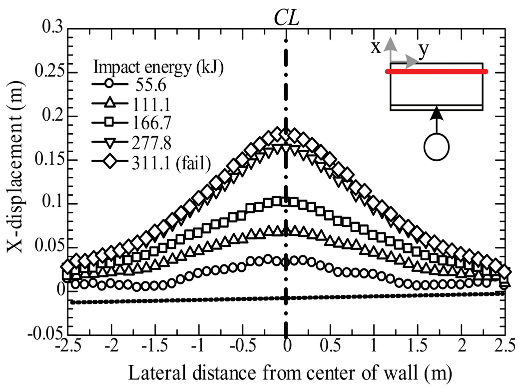

Figure 13. The maximum displacement of protecting wall according to given impact energy.

On the other hand, the results using elasto-perfect plastic model for protecting wall are more fit with those of experiment than the other material models in the case of type 2 and 3. This means that elastic model can't express large deformation of protecting wall such as type 2 and 3.

4.3 *The effect of impact energy and impact point*

Numerical analyses with elasto-perfectly plastic model are carried out to investigate the effect of impact energy at same impact point (a middle of protecting wall) and weight of rockfall (4.9 kN) for type 1.

Figure 12 represents the maximum impact load according to given impact energy. Calculation is impossible at about 300 kJ of impact energy and 1500 kN of impact load. These load and energy mean limit value in this protecting wall against rockfall.

Figure 13 shows the displacement along to the horizontal direction on top face of protecting wall

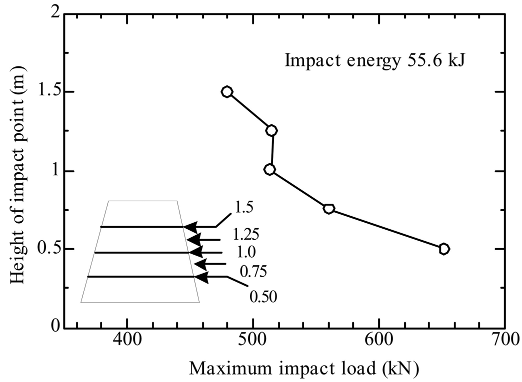

Figure 14. The maximum load according to given impact point in protecting wall (impact energy 55.6 kJ).

according to impact energy. The effect region and maximum displacement increase by impact energy. The effect distance of displacement is about 3 m in the case of impact energy 55.6 kJ. On the other hand, all parts on top face of protecting wall are influenced and amount of displacement become also larger according to the increase of the impact energy.

Figure 14 shows the effect of impact point in the protecting wall with impact energy 55.6 kJ. Although same impact energy is applied to each impact point, the value of impact load of rockfall is different.

In the case of impact point 0.5 m, the load is the largest than those of other impact point due to the fixed boundary condition and weight of protecting wall above impact point. On the other hand, in the case of high impact point such as 1.5 m, the impact load of rockfall become small due to the large deformation of wall.

5 CONCLUSION

Full-scale field tests and numerical analyses were carried out to investigate the interaction problem between a rockfall and a protecting wall. The influences of impact load and impact point on the stability of protecting wall were also investigated. From the results of the full-scale field tests and numerical analyses, the following conclusions are obtained:

(1) The efficiency of protecting wall against rockfall is very different according to the material used.
(2) Although the protecting wall using ground material indicates larger deformation than concrete wall, it can be used for low rockfall energy by its economic advantage and convenient repair.
(3) Numerical analyses with optimized material parameters reproduced experimental results quantitatively.

(4) A limit capacity of a protecting wall against rockfall can be calculated by numerical analyses.
(5) The calculated impact load is different according to the different impact point in the wall.

REFERENCES

Prisco, C. DI. & Vecchiotti, M. 2006. A rheological model for the description of boulder impacts on granular strata. *Geotechnique* 56, No. 7: 469–482

Hallquist, J. O. 2003. *LS-DYNA Theoretical Manual V.970.* Livermore, CA: Livermore Software Technology Corporation

Wu, W. & Thomson, R. 2007. A study of the interaction between a guardrail post and soil during quasi-static and dynamic loading. *Int. Jour. Impact engineering* 34: 883–898